SUPPLEMENTARY INFORMATION

Effect of trimetallization in thiolate-protected $Au_{24-n}Cu_nPd$ clusters

Sachil Sharma,[a] Wataru Kurashige,[a] Katsuyuki Nobusada[b,c] and Yuichi Negishi*[a,d,e]

[a] *Department of Applied Chemistry, Faculty of Science, Tokyo University of Science, 1-3 Kagurazaka, Shinjuku-ku, Tokyo 162−8601, Japan. Fax: +81−3−5261−4631; Tel: +81−3−5228−9145; E-mail: negishi@rs.kagu.tus.ac.jp*

[b] *Department of Theoretical and Computational Molecular Science, Institute for Molecular Science, Myodaiji, Okazaki, Aichi 444−8585, Japan.*

[c] *Elements Strategy Initiative for Catalysts and Batteries (ESICB), Kyoto University, Katsura, Kyoto 615−8520, Japan.*

[d] *Department of Materials Molecular Science, Institute for Molecular Science, Myodaiji, Okazaki, Aichi 444−8585, Japan.*

[e] *Photocatalysis International Research Center, Tokyo University of Science, 2641 Yamazaki, Noda, Chiba 278−8510, Japan.*

Table S1. Maximum number of Cu atoms in $Au_{25-n}Cu_n(SC_2H_4Ph)_{18}$ bimetallic clusters and $Au_{24-n}Cu_nPd(SC_2H_4Ph)_{18}$ trimetallic clusters.

Initial metal ion ratios Au:Cu:Pd	Maximum number of Cu atoms in $Au_{25-n}Cu_n(SC_2H_4Ph)_{18}$	Maximum number of Cu atoms in $Au_{24-n}Cu_nPd(SC_2H_4Ph)_{18}$
23:1:1	5 [a]	2 [a]
22:1:2	4 [a]	3 [a]
21:1:3	3 [a]	2 [a]
20:1:4	3 [a]	2 [a]
19:1:5	4 [a]	2 [a]
18:1:6	5 [a]	3 [a]
22:2:1	5 [b]	3 [b]
21:2:2	6 [b]	2 [b]
20:2:3	4 [b]	2 [b]
19:2:4	4 [b]	2 [b]
18:2:5	6 [b]	3 [b]
18:3:4	8 [c]	3 [c]

[a] These values are from Figure S11. [b] These values are from Figure S12. [c] These values are from Figure S13.

Table S2. Results of DFT calculations for $Au_{23}CuPd(SCH_3)_{18}$.

Cu site	Relative energy (eV)	HOMO–LUMO gap (eV)
Surface [a]	0.00	1.32
Staple [a]	0.21	1.33

[a] These structures are shown in Scheme 1(b)(c).

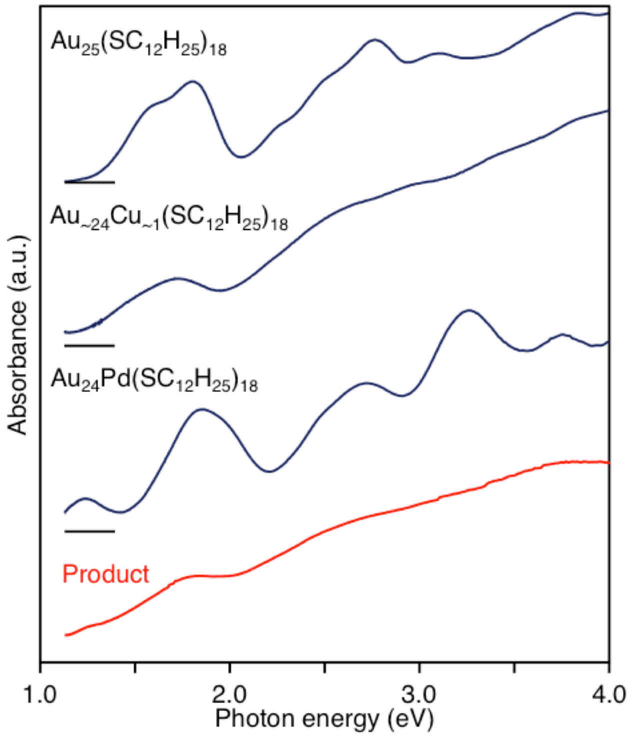

Figure S1. Optical absorption spectrum of a product (red curve), which was obtained with a $HAuCl_4$:$Cu(C_5H_7O_2)_2$:$PdCl_2{\cdot}2NaCl$ concentration ratio of 23:1:1. The optical absorption spectra of $Au_{25}(SC_{12}H_{25})_{18}$,[1] $Au_{\sim24}Cu_{\sim1}(SC_{12}H_{25})_{18}$, which was reported in this study, and $Au_{24}Pd(SC_{12}H_{25})_{18}$[2] are also shown for comparison purposes.

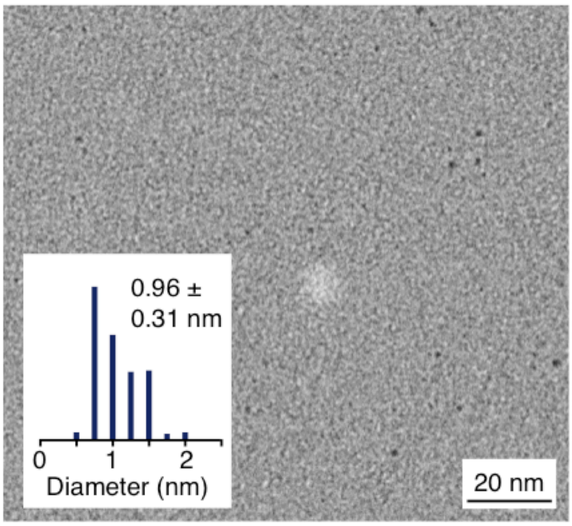

Figure S2. TEM image and corresponding particle size distribution of a product, which was obtained with a $HAuCl_4$:$Cu(C_5H_7O_2)_2$:$PdCl_2{\cdot}2NaCl$ concentration ratio of 23:1:1.

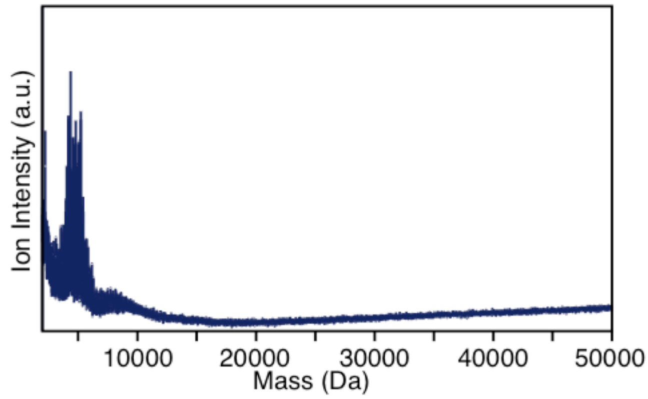

Figure S3. Negative-ion MALDI mass spectrum of a product, which was obtained with a $HAuCl_4$:$Cu(C_5H_7O_2)_2$:$PdCl_2$·2NaCl concentration ratio of 23:1:1. In this experiment, mass spectrum was observed with a fluence higher than that used for the observation of non-destructive mass spectra to confirm the absence of the larger clusters.

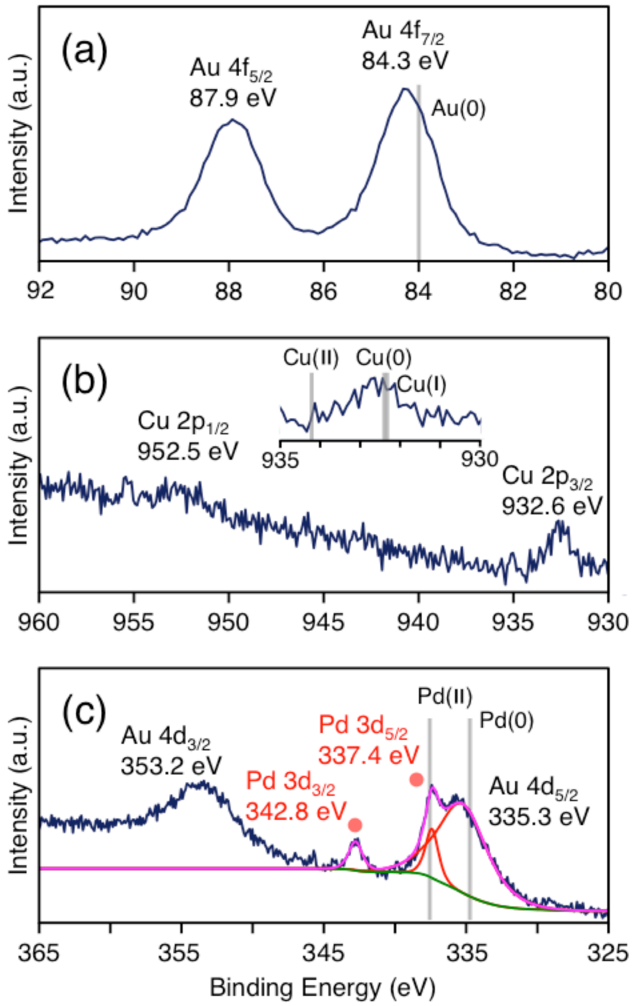

Figure S4. (a) Au 4f, (b) Cu 2p, and (c) Pd 3d X-ray photoelectron spectra of a product, which was obtained with a $HAuCl_4$:$Cu(C_5H_7O_2)_2$:$PdCl_2$·2NaCl concentration ratio of 23:1:1.

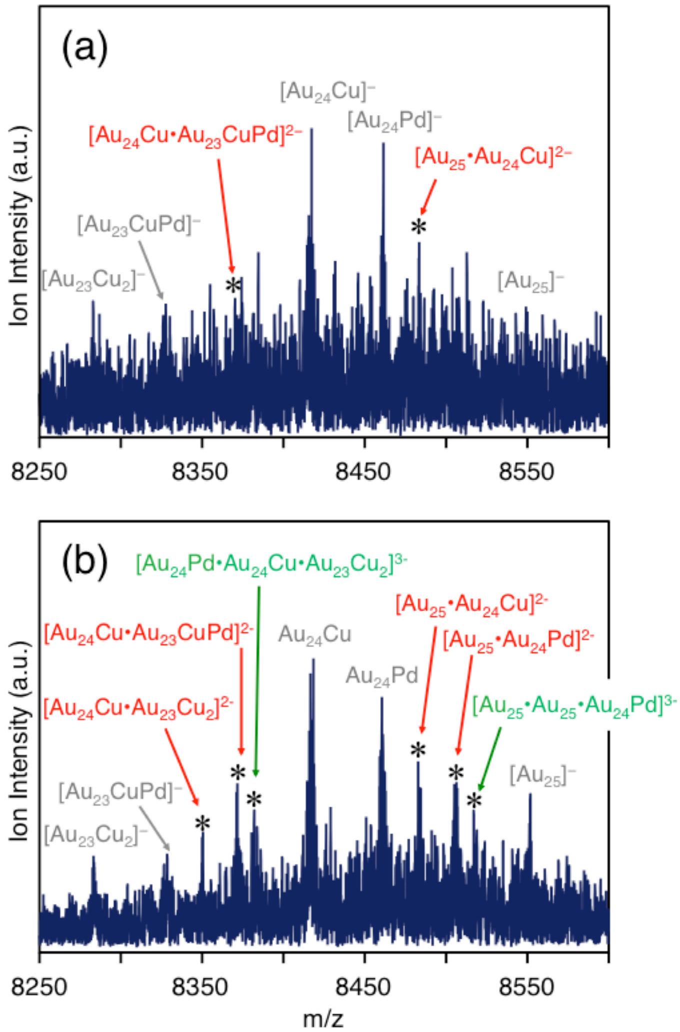

Figure S5. Assignments of peaks (denoted by *) observed in the negative-ion ESI mass spectra of a mixture of $Au_{24-n}Cu_nPd(SC_{12}H_{25})_{18}$ and $Au_{25-n}Cu_n(SC_{12}H_{25})_{18}$ (a) following extraction and (b) after standing for 1 h at room temperature in toluene. The peaks (denoted by *) are attributed to the dianion of cluster dimers or the trianion of cluster trimers, which are sometimes observed in the ESI mass spectra.[3] Only the number of the metal atoms and the charge states are shown for simplicity.

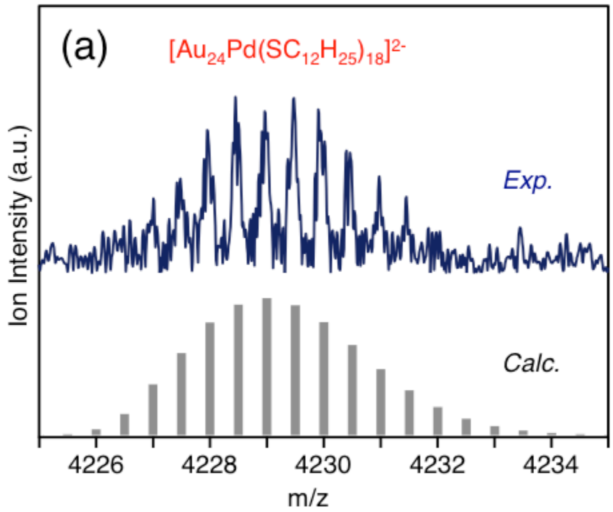

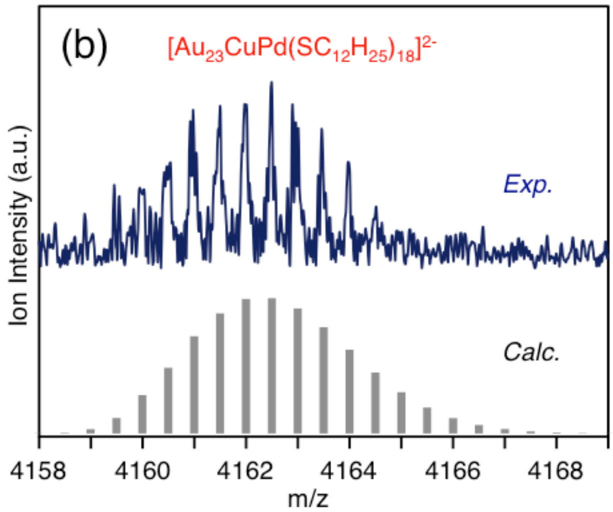

Figure S6. Isotope patterns of the peaks of (a) $[Au_{24}Pd(SC_{12}H_{25})_{18}]^{2-}$ and (b) $[Au_{23}CuPd(SC_{12}H_{25})_{18}]^{2-}$ observed in ESI mass spectrum of Figure 2(a) together with those of the calculation. Isotope patterns were calculated using "Isotope Pattern Simulator" software.

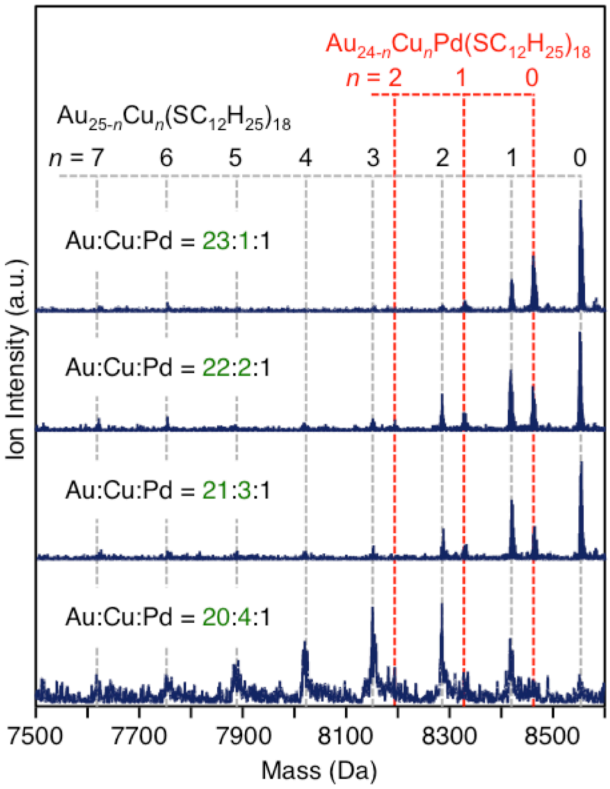

Figure S7. Negative-ion MALDI mass spectra of samples synthesized with various ratios of $[Cu(C_5H_7O_2)_2]$:$[HAuCl_4]$. The ratio of $[PdCl_2{\cdot}2NaCl]$ was fixed such that $[HAuCl_4]$:$[Cu(C_5H_7O_2)_2]$:$[PdCl_2{\cdot}2NaCl]$ = x:y:1, where $x + y = 24$ (Table 1).

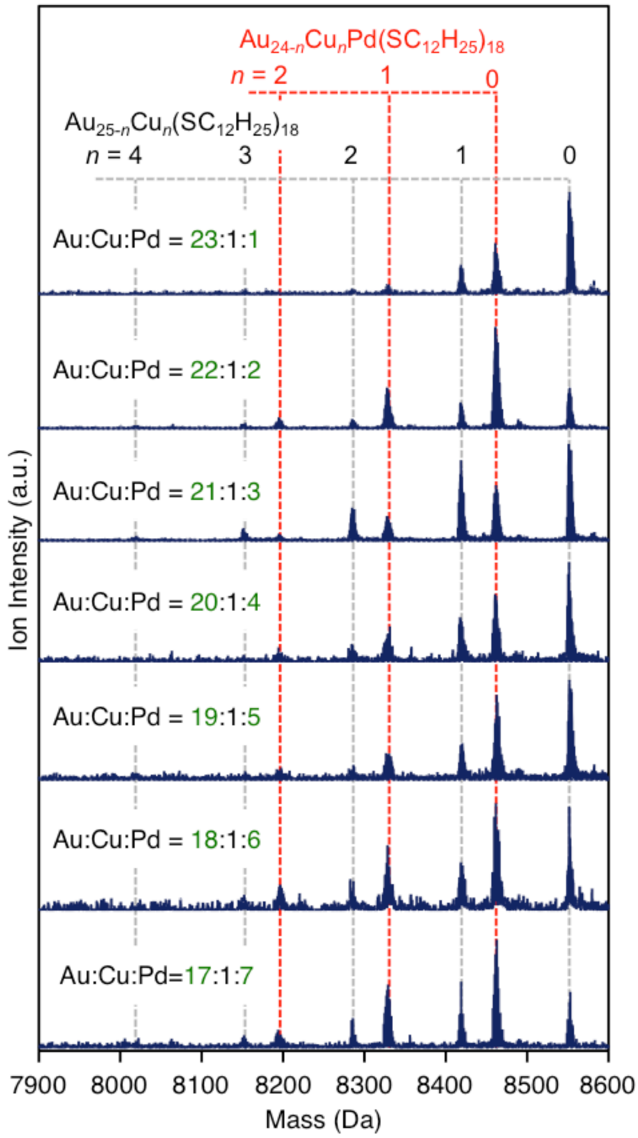

Figure S8. Negative-ion MALDI mass spectra of samples synthesized with various ratios of $[PdCl_2{\cdot}2NaCl]$:$[HAuCl_4]$. The ratio of $[Cu(C_5H_7O_2)_2]$ was fixed such that $[HAuCl_4]$:$[Cu(C_5H_7O_2)_2]$:$[PdCl_2{\cdot}2NaCl]$ = x:1:z, where $x + z = 24$ (Table 1).

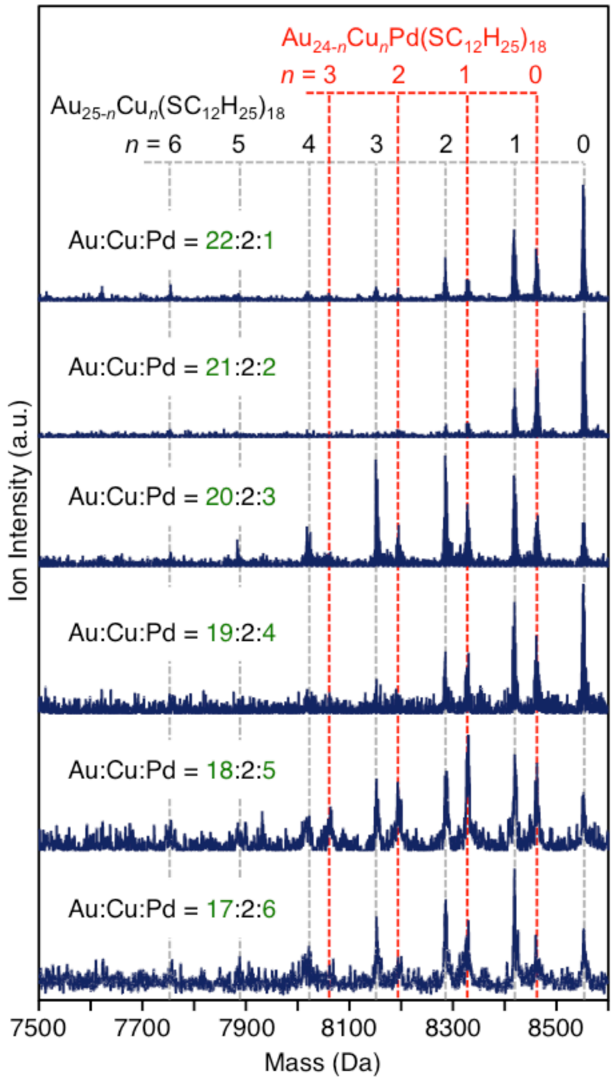

Figure S9. Negative-ion MALDI mass spectra of samples synthesized with various ratios of [$PdCl_2$·2NaCl]:[$HAuCl_4$]. The ratio of [$Cu(C_5H_7O_2)_2$] was fixed such that [$HAuCl_4$]:[$Cu(C_5H_7O_2)_2$]:[$PdCl_2$·2NaCl] = x:2:z, where $x + z = 23$ (Table 1).

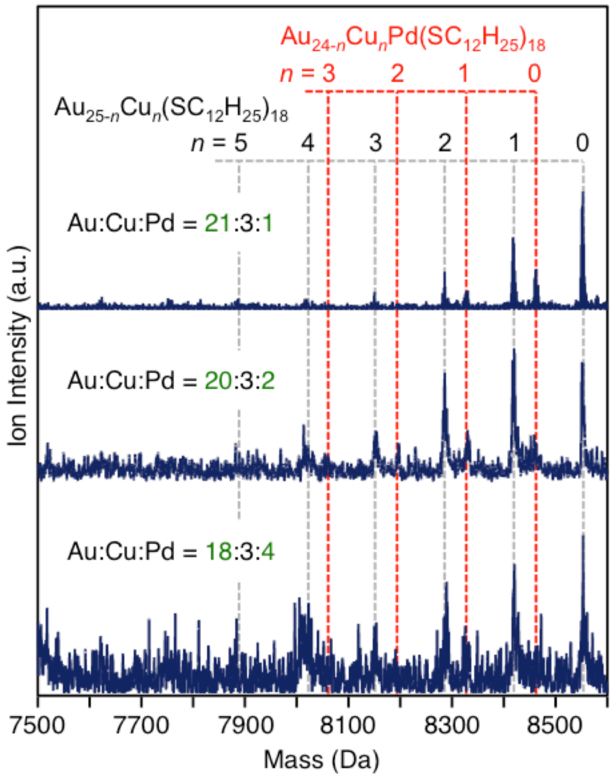

Figure S10. Negative-ion MALDI mass spectra of samples synthesized with various ratios of $[PdCl_2{\cdot}2NaCl]$:$[HAuCl_4]$. The ratio of $[Cu(C_5H_7O_2)_2]$ was fixed such that $[HAuCl_4]$:$[Cu(C_5H_7O_2)_2]$:$[PdCl_2{\cdot}2NaCl]$ = x:3:z, where $x + z = 22$ (Table 1).

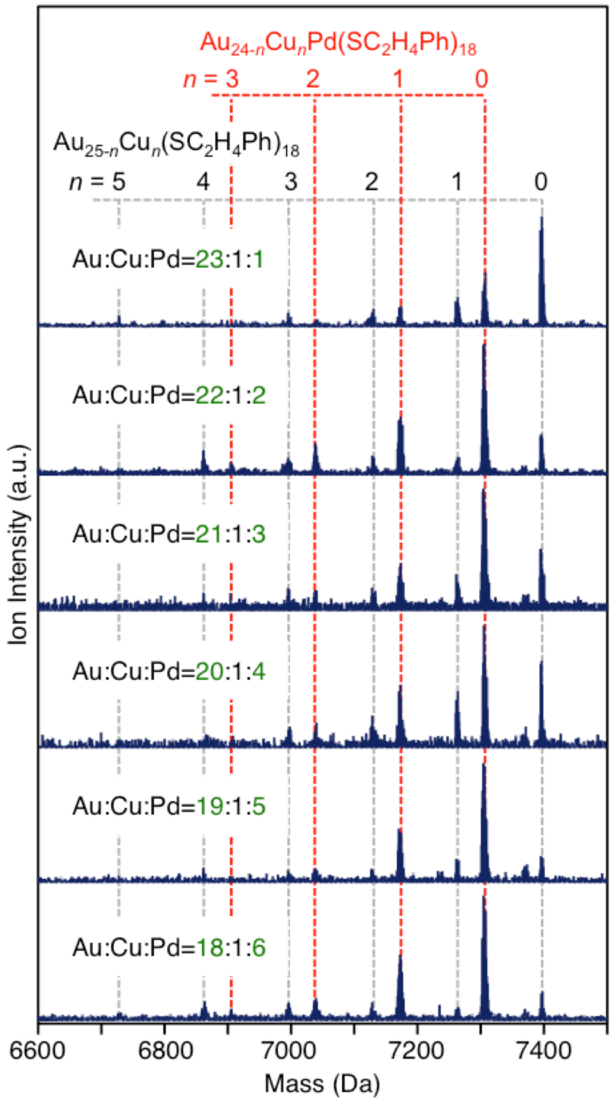

Figure S11. Negative-ion MALDI mass spectra of samples synthesized with various ratios of $[PdCl_2 \cdot 2NaCl]$:$[HAuCl_4]$ for 25-metal atom clusters protected by phenylethanethiolate (a mixture of $Au_{25-n}Cu_n(SC_2H_4Ph)_{18}$ and $Au_{24-n}Cu_nPd(SC_2H_4Ph)_{18}$). The ratio of $[Cu(C_5H_7O_2)_2]$ was fixed such that $[HAuCl_4]$:$[Cu(C_5H_7O_2)_2]$:$[PdCl_2 \cdot 2NaCl]$ = x:1:z, where $x + z = 24$ (Table S1).

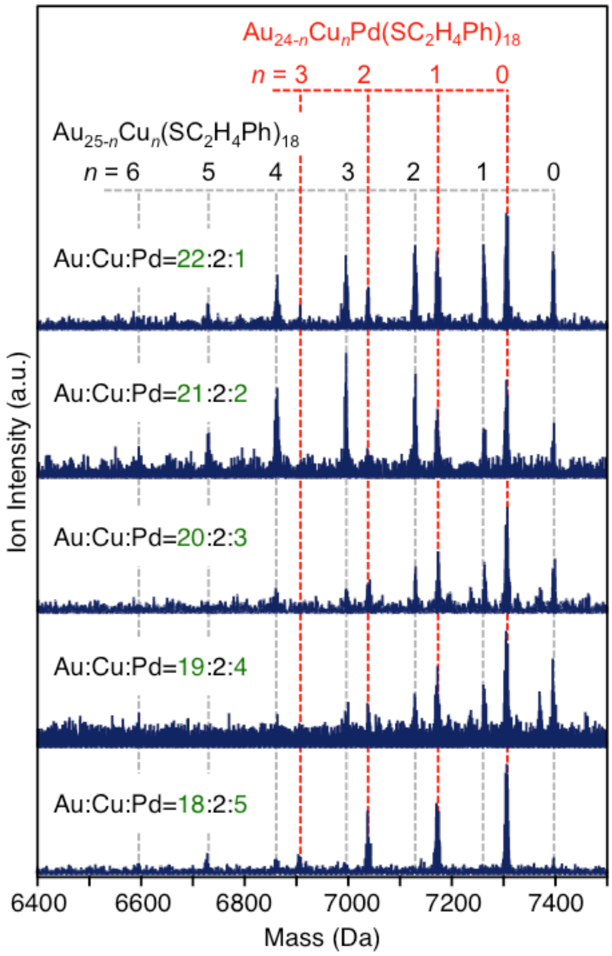

Figure S12. Negative-ion MALDI mass spectra of samples synthesized with various ratios of $[PdCl_2{\cdot}2NaCl]$:$[HAuCl_4]$ for 25-metal atom clusters protected by phenylethanethiolate (a mixture of $Au_{25-n}Cu_n(SC_2H_4Ph)_{18}$ and $Au_{24-n}Cu_nPd(SC_2H_4Ph)_{18}$). The ratio of $[Cu(C_5H_7O_2)_2]$ was fixed such that $[HAuCl_4]$:$[Cu(C_5H_7O_2)_2]$:$[PdCl_2{\cdot}2NaCl]$ = x:2:z, where $x + z = 23$ (Table S1).

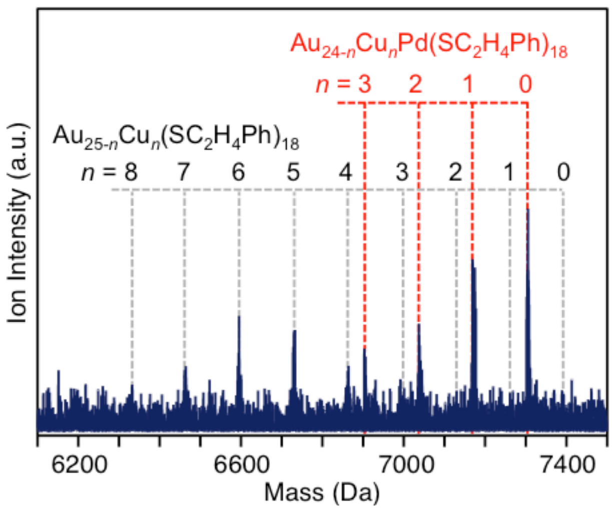

Figure S13. Negative-ion MALDI mass spectrum of sample synthesized from a mixture of $Au_{25-n}Cu_n(SC_2H_4Ph)_{18}$ and $Au_{24-n}Cu_nPd(SC_2H_4Ph)_{18}$ with $[HAuCl_4]$:$[Cu(C_5H_7O_2)_2]$:$[PdCl_2{\cdot}2NaCl]$ = 18:3:4 (Table S1).

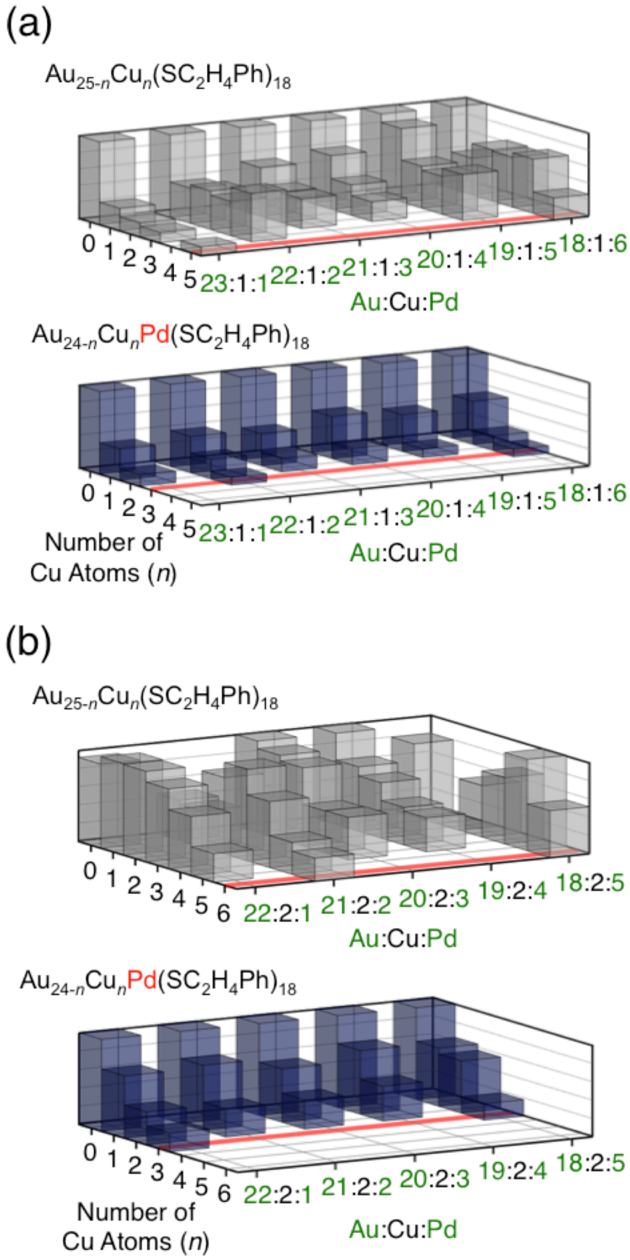

Figure S14. Correlation between the number of Cu atoms in clusters and the relative ion intensity in the mass spectra for $Au_{25-n}Cu_n(SC_2H_4Ph)_{18}$ and $Au_{24-n}Cu_nPd(SC_2H_4Ph)_{18}$ synthesized with various ratios of $[PdCl_2 \cdot 2NaCl]$:$[HAuCl_4]$. The ratio of $[Cu(C_5H_7O_2)_2]$ was fixed such that $[HAuCl_4]$:$[Cu(C_5H_7O_2)_2]$:$[PdCl_2 \cdot 2NaCl]$ was (a) x:1:z, where $x + z = 24$ (Figure S11), or (b) x:2:z, where $x + z = 23$ (Figure S12). The red lines indicate the maximum number of Cu atoms in the cluster determined in a series of experiments.

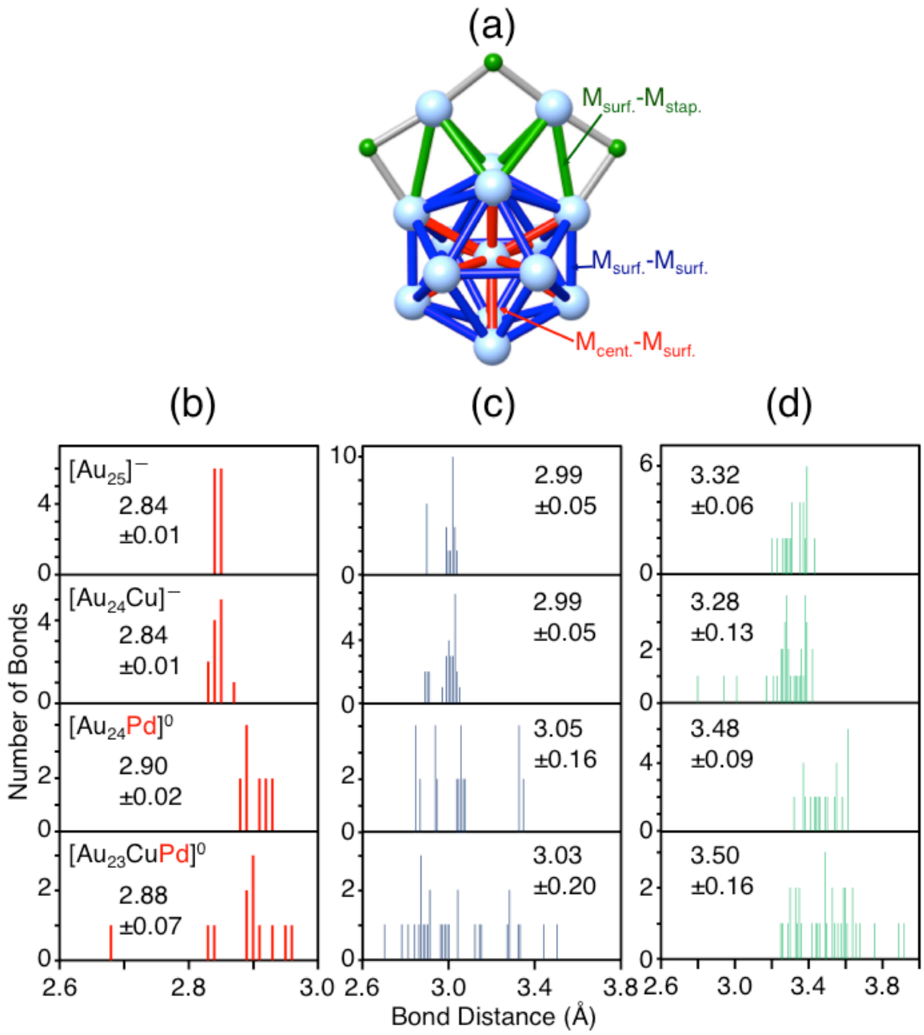

Figure S15. (a) Anatomy of 25 metal atom cluster highlighting three kinds of bond. (b)−(d) Histograms of the intermetallic bond length in $[Au_{25}(SCH_3)_{18}]^-$, $[Au_{24}Cu(SCH_3)_{18}]^-$, $[Au_{24}Pd(SCH_3)_{18}]^0$, and $[Au_{23}CuPd(SCH_3)_{18}]^0$ in which one Au atom on the surface of $[Au_{24}Pd(SCH_3)_{18}]^0$ is replaced with Cu (Scheme 1(c)); (b) $M_{cent.}$−$M_{surf.}$, (c) $M_{surf.}$−$M_{surf.}$ and (d) $M_{surf.}$−$M_{stap.}$.

References

1. Y. Negishi, N. K. Chaki, Y. Shichibu, R. L. Whetten and T. Tsukuda, *J. Am. Chem. Soc.*, 2007, **129**, 11322–11323.
2. Y. Negishi, W. Kurashige, Y. Niihori, T. Iwasa and K. Nobusada, *Phys. Chem. Chem. Phys.*, 2010, **12**, 6219–6225.
3. W. Kurashige, S. Yamazoe, M. Yamaguchi, K. Nishido, K. Nobusada, T. Tsukuda and Y. Negishi, *J. Phys. Chem. Lett.*, 2014, **5**, 2072–2076.